

HIGH-REDSHIFT SUPERWINDS AS THE SOURCE OF THE STRONGEST Mg II ABSORBERS: A FEASIBILITY ANALYSIS¹

NICHOLAS A. BOND, CHRISTOPHER W. CHURCHILL², JANE C. CHARLTON³

Department of Astronomy and Astrophysics
The Pennsylvania State University
University Park, PA 16802
bond, cwc, charlton@astro.psu.edu

AND

STEVEN S. VOGT²
UCO/Lick Observatories
Board of Studies in Astronomy and Astrophysics
University of California, Santa Cruz, CA 96054
vogt@ucolick.org

Draft version December 3, 2018

ABSTRACT

We present HIRES/Keck profiles of four extremely strong ($W_r > 1.8 \text{ \AA}$) Mg II absorbers at $1 < z < 2$. The profiles display a common kinematic structure, having a sharp drop in optical depth near the center of the profile and strong, black-bottomed absorption on either side. This “symmetric-inverted” structure, with a velocity spread of several hundred kilometers per second, is suggestive of superwinds arising in actively star-forming galaxies. Low-ionization absorption of similar strength has been observed in local star-forming galaxies.

The Mg II absorbers with $W_r > 1.8 \text{ \AA}$ evolve away from $z = 2$ to the present. We propose that a substantial fraction of these very strong absorbers are due to superwinds and that their evolution is related to the redshift evolution of star-forming galaxies. Based on the observed redshift number density of $W_r > 1.8 \text{ \AA}$ Mg II absorbers at $1 < z < 2$, we explore whether it is realistic that superwinds from starbursting galaxies could give rise to these absorbers. Finally, we do an analysis of the superwind connection to damped Ly α absorbers (DLAs). DLAs and superwinds evolve differently and usually have different kinematic structure, indicating that superwinds probably do not give rise to the majority of DLAs.

Subject headings: quasars: absorption lines — interstellar medium — superbubbles

1. INTRODUCTION

The very strong ($W_r(2796) > 1.8 \text{ \AA}$), $z > 1$ Mg II absorbers are of great interest in determining the nature of the high-column-density and/or high-velocity material present in the early universe. At low redshift, very strong Mg II systems evolve away as $(1+z)^{2.24}$ (Steidel & Sargent 1992). This evolution parallels the star formation history of the universe (e.g. Yan et al. 1999), suggesting a link between Mg II absorption and star formation activity (e.g. Guillemin & Bergeron 1997, Churchill et al. 1999). The disappearance of these absorbers at low redshifts also suggests that the gas giving rise to the absorbers has dispersed and/or changed state with time. Both of these factors suggest a connection between very strong Mg II absorbers and superwinds in starburst galaxies.

Star formation in the nucleus of a starburst galaxy is thought to give rise to a superbubble, a hollow shell of swept-up ISM gas (e.g. Mac Low & McCray 1988). If this superbubble expands sufficiently to escape the galaxy’s potential well, it can “blow out” into the halo of the galaxy. At this point, Rayleigh–Taylor instabilities would cause the shell to fragment and the superbubble would begin to vent hot material into the halo of the starbursting galaxy, forming a bipolar, weakly-collimated outflow (e.g., Tomisaka & Bregman 1993; Suchkov 1994; Strickland 1998; Tenorio-Tagle & Munoz-Tunon 1998).

The central region of the superwind/superbubble is very hot ($T \sim 10^7 \text{ K}$) and gives rise to X-ray emission. There may be a conduction zone between the shell and the central region with coronal gas ($T \sim 10^5 \text{ K}$) that exhibits absorption in high-ionization UV lines (e.g. CIV and OVI). The superwind/superbubble shell, however, is cold ($T \sim 10^4 \text{ K}$) and exhibits low-ionization absorption in Na I $\lambda\lambda 5890, 5896$ (Heckman et al. 2000), indicating that Mg II absorption would also be present. Some material associated with the cold phase emits in H α because of the ionizing flux coming from the young stars. Rayleigh–Taylor instabilities would result in clumping of the cold material and a line of sight through these clumps would be expected to show kinematically complex absorption.

Heckman et al. (2001) observe the absorption spectrum of a dwarf galaxy, NGC 1705, at high resolution with *FUSE*. There is evidence for a 100 km s^{-1} outflow with both cold and warm phases of gas. Kinematically, the warm phase seems consistent with an expanding superbubble (the beginnings of a superwind). Rather than simply having the warm phase in a conduction zone, however, Heckman et al. (2001) hypothesize that hot gas is blowing out through the shell and mixing with the cold gas. This process creates warm gas of $\sim 10^5 \text{ K}$ gas that gives rise to OVI absorption. The cold phase, on the other hand, is expected to arise in the shell. The absorption lines near the systemic velocity of NGC 1705 show $\sim 100 \text{ km s}^{-1}$ spreads.

¹Based in part on observations obtained at the W. M. Keck Observatory, which is operated as a scientific partnership among Caltech, the University of California, and NASA. The Observatory was made possible by the generous financial support of the W. M. Keck Foundation.

²Visiting Astronomer, W. M. Keck Observatory

³Center for Gravitational Physics and Geometry

In this paper, we argue that a substantial fraction of the $W_r > 1.8 \text{ \AA}$ Mg II absorption systems are produced by superwinds. In § 2, we present several HIRES/Keck absorption profiles of very strong, $z > 1$ Mg II absorbers. In § 3, we establish the basis for our hypothesis that superwinds give rise to Mg II absorption systems like the ones in our sample. In § 4, we calculate the expected redshift number density, $N(z)$ of these absorbers if they are caused by superwinds. In § 5, we assess the uncertainty of the parameters going into the $N(z)$ calculation. In § 6, we briefly discuss the implications for Lyman break galaxies and damped Ly α absorbers (DLAs). Finally, in § 7, we summarize our results and conclusions.

2. DATA AND ANALYSIS

2.1. Sample Selection and Observations

During the observing runs for a larger program to study the kinematics of Mg II absorbers at $0.5 < z < 1.5$ (Churchill, Steidel, & Vogt 1996; Charlton & Churchill 1998; Churchill et al. 1999; Churchill & Vogt 2001), several very large equivalent width systems ($W_r > 1.8 \text{ \AA}$) were observed at $z > 1$. The goal was to obtain a small sample of kinematic data from systems belonging to the strongly evolving population of $W_r > 1.8 \text{ \AA}$ Mg II absorbers documented by Steidel & Sargent (1992).

Four Mg II systems were targeted in three quasars. The systems, shown in Figure 1 are at $z = 1.1745$ toward Q 0450–132, $z = 1.3201$ and $z = 1.5541$ toward Q 1213–003, and $z = 1.7948$ toward B2 1225 + 317. The latter system was studied in detail at high spectral resolution by Bechtold et al. (1987).

The four quasars were observed with the HIRES spectrometer (Vogt et al. 1994) on the Keck I telescope on the night of 24 January 1995 UT. HIRES was configured in first-order using the $0.861''$ slit width and either the $7''$ or $14''$ decker. Because of the first-order HIRES format, there are small gaps in the spectral coverage red-ward of 5100 \AA , where the free spectral range exceeds the width of the 2048×2048 Tektronix CCD. The spectral resolution is $R = 45,000$ ($\simeq 6.6 \text{ km s}^{-1}$).

The journal of observations is presented in Table 1, which lists, for each quasar, the V magnitude, emission redshift, observation date, total integration time, wavelength coverage (not including gaps above 5100 \AA), decker size for sky subtraction, and high pass filter for 2nd-order blocking. Three separate, consecutive integrations were obtained for each quasar spectrum, bracketed by Th–Ar calibration lamps.

2.2. Data Reduction and Analysis

The HIRES data were reduced with the IRAF⁴ APEXTRACT package (V2.10.3) for echelle data. Each observed data frame was overscan subtracted, bias frame corrected, scattered light corrected, and flat-fielded in the standard fashion. The data have been calibrated to vacuum wavelengths and converted to heliocentric velocity. The unfluxed continuum was normalized using the methods described by Sembach & Savage (1992). Further details of the data reduction can be found in Churchill (1997); Churchill et al. (1999), Churchill et al. (2000), and Churchill & Vogt (2001).

Equivalent widths and equivalent width limits were computed using the methods of Lanzetta, Wolfe, & Turnshek (1987). We focus on the Mg II, Fe II, Mg I, and Mn II transitions because they are represented for all four systems (due to a combination of their redshifted wavelengths and the wave-

length coverage of the HIRES echelle). The apparent optical depth (AOD, Savage & Sembach 1991) column densities, N_a , were also computed for each atom/ion. The N_a values were determined by combining information from all unsaturated transitions as described in the appendix of Churchill & Vogt (2001). When limits are placed, they are simply the measured N_a of the weakest transition (i.e. no correction for unresolved saturation is applied; Jenkins 1996).

In Table 2, we list the equivalent widths or their limits (3σ), and the adopted AOD column densities for each system. We also present the total velocity width, using the velocity range over which the equivalent widths were computed.

3. SUPERWIND HYPOTHESIS

We hypothesize that the profiles presented in Figure 1 arise in a quasar spectrum when the line of sight passes through the outflowing gas of a superwind. There are several distinctive features of the profiles that can be easily explained with this hypothesis: 1) a narrow ‘‘inversion’’ (an anomalous region of low optical depth) at kinematic center, 2) many absorption components spread out over a large velocity range ($\sim 250 \text{ km s}^{-1}$), and 3) a variation in cloud-to-cloud abundance patterns.

The most prominent feature is the inversion at the center of the profile. This type of feature implies that the absorbing material is either expanding outward or falling inward, with little or no material moving at the systemic velocity of the absorbing medium. The outflows of superwinds behave in this way, typically forming a double-cone structure that is symmetric about the minor axis of the host galaxy (e.g. Heckman, Armus, & Miley 1990). If a quasar line of sight were to pass through both cones, one would see blue-shifted absorption from one cone and red-shifted absorption from the other cone. If the galaxy inclination was very close to face-on, there might be absorption from the disk at the systemic velocity, but face-on orientations are rare and the disk absorption would be blue- or red-shifted at other inclinations. The inversion could also be created by passing through a single cone of a superwind. Most of the Mg II absorption is created in the cold shell along the edges of the outflow. The center of the wind, which would correspond to the center of the profile, is mostly filled with hot ($\sim 10^6 \text{ K}$) gas and would not create much Mg II absorption.

A typical velocity spread for these systems is $\sim 250 \text{ km s}^{-1}$. This is consistent with the typical superwind velocities, which are observed to be between 100 and 1000 km s^{-1} (e.g. Heckman et al. 2000). In fact, Heckman et al. (2001, in prep) have observed the Mg II absorption from a known superwind, NGC1705. They use the starburst region itself as a continuum and are looking through only one side of the wind, so we expect that they should measure about half the velocity spread of the very strong Mg II absorbers in our sample. They find $\Delta v \sim 150 \text{ km s}^{-1}$, a spread consistent with our data.

Another feature of the profiles that is immediately obvious is the many absorption components. Weak transitions, like those of Mg I and Fe II, clearly show that the saturated troughs seen in Mg II are made up of many components in velocity space. In the context of the superwind model, these clouds most likely correspond to the fragmented pieces of the entrained material. These fragments are produced by Rayleigh–Taylor instabilities in the shell of the initial superbubble when it blows out of the host galaxy. The shell pieces are then entrained and become dispersed along the edges of the weakly-collimated outflow,

⁴IRAF is distributed by the National Optical Astronomy Observatories, which are operated by AURA, Inc., under contract to the NSF.

producing the multi-component absorption troughs.

The final feature that stands out in Figure 1, particularly in the $z = 1.1746$ system in Q0450 – 132, is the variation in cloud-to-cloud line ratios. For example, in the Q0450 – 132 system, the ratio of the line strengths of FeII and MnII varies dramatically across the profile. Since these species have similar recombination rates and photoionization cross sections, this indicates that the abundance patterns of the gas varies from cloud to cloud. This kind of behavior might be expected in a superwind if the fragments of entrained material causing the absorption originated in different regions of the ISM of the pre-starburst galaxy, each populated with different abundance patterns.

3.1. Alternative Explanations

An alternative hypothesis as to the origin of the very strong MgII absorbers was put forth by Danks et al. (2001). Based on absorption profiles from the regions surrounding the Carinae Nebula, they suggest that some very strong MgII absorption could be due to interstellar gas in the vicinity of active star formation regions. Unlike in the superwinds, however, the gas in these nebulae is very cold—there is very little warm gas. Therefore, observations of high-ionization transitions, like CIV, would help confirm or refute this hypothesis. In addition, these nebulae would be expected to exhibit variability, as seen in the Carinae Nebula, over timescales of a few years. However, in the superwind scenario, even if the clouds were as small as 1 pc in size and moving at velocities of a few hundred km s^{-1} , we would expect observable variability over timescales of no less than 10^3 or 10^4 years. Multi-epoch observations of the very strong MgII systems are required to determine whether interstellar gas could be the source of the absorption.

A further possibility for the origin of these absorbers is a pair of galaxies in a group or cluster or a large galaxy and its satellite (Churchill 1999). Although there may be enough of these pairs to explain the frequency of the “symmetric-inverted” systems, they do not provide as natural an explanation for the kinematics. If this absorption was due solely to galaxies, one would expect to observe many more systems with single saturated troughs surrounded by a significant number of small outlying clouds. Also, the splitting of the troughs in velocity space shows remarkably little variation. One would expect pairs of galaxies to show a larger range of velocity differences.

3.2. Q1213 – 0017 Field

The field of the quasar Q1213 – 0017 has been the target of extensive ground-based and *HST* imaging in the optical and near-IR (Liu et al. 2000). To date, four galaxies have been found within ~ 1 Mpc of the quasar at $z \sim 1.3$, the redshift of one of the intervening strong MgII absorbers in the quasar spectrum. The closest of these galaxies is at an impact parameter⁵ of 195 kpc and is unlikely to be responsible for the MgII absorption at that redshift. However, the abundance of bright galaxies at this redshift is indicative of a cluster and there are a few fainter objects in the field that could not be studied spectroscopically. If these objects are at $z \sim 1.3$, they could be causing the absorption.

In the superwind scenario, we would expect the majority of $W_r > 1.8 \text{ \AA}$ MgII absorption systems to arise in relatively low-luminosity galaxies below the detection threshold of the Q1213 – 0017 images. For example, NGC1705 would not be

detected in the images of Liu et al. (2000). Because there is a cluster near the redshift of the absorption system it is not unreasonable to think that the line of sight is passing through the wind of a low-luminosity starburst or a relic outflow.

4. FEASIBILITY ANALYSIS

We wish to determine the feasibility of our hypothesis that superwinds give rise to these very strong “symmetric-inverted” MgII systems at high redshift. To do this, we first estimate the observed redshift number density, $N(z)$, of MgII absorbers with $W_r > 1.8 \text{ \AA}$ at $\langle z \rangle \sim 1.3$ from quasar absorption line surveys. Then, we explore the plausible range of $N(z)$ of these absorbers assuming they are superwinds associated with starburst galaxies. In performing this calculation, we parameterize the physical properties of superwinds and find the parameter space consistent with the observed $N(z)$ of very strong symmetric-inverted MgII systems.

4.1. Observed $N(z)$ of Very Strong MgII Systems

As can be seen in Figure 2 of Steidel & Sargent (1992), the observed $N(z)$ of $W_r > 1 \text{ \AA}$ MgII absorption systems is ~ 0.3 . The statistics were not sufficient to determine an $N(z)$ for a higher minimum W_r , so we can only place a limit on the $N(z)$ of $W_r > 1.8 \text{ \AA}$ systems, $N(z) < 0.3$. We can approximate the actual value by making an extrapolation of the curve. After doing this, we get $N(z) \sim 0.15$ and use this value in the calculations below. Although the exact value of $N(z)$ is uncertain, the following calculation is rough and nature and a slightly different value will not affect our conclusions.

4.2. Estimated $N(z)$ of Absorbing Superwinds

For an absorber with number density $n(z)$ and cross section $\sigma(z)$, the number of absorbers per unit redshift path is

$$N(z) = \frac{c n(z) \sigma(z)}{H_0} (1+z) (1+2q_0 z)^{1/2}. \quad (1)$$

The cross section and density cannot be determined independently. Assuming the absorption is associated with a population of galaxies at $z = 1.3$, the product of the two can be obtained by integrating

$$n \sigma = C_f C_t \int_{L_{min}}^{\infty} \phi(L/L^*) \pi R(L/L^*)^2 dL, \quad (2)$$

where C_f is the covering factor, C_t is a time-scale factor explained below, and L_{min} is the minimum H α luminosity that a galaxy can have and still give rise to symmetric-inverted MgII absorption. We used $\phi(L/L^*) = \Phi^* (L/L^*)^\alpha e^{-L/L^*}$, a Schechter formulation of a galaxy luminosity function (Schechter 1976), and $R(L/L^*) = R^* (L/L^*)^\beta$, a Holmberg formulation of a radius-luminosity relationship (Holmberg 1975), where R^* is the radius out to which one gets very strong absorption in an L^* galaxy.

When the integration is carried out, one obtains

$$n \sigma = C_f C_t \Phi^* \pi R_*^2 \Gamma(\alpha + 2\beta + 1, L_{min}/L^*), \quad (3)$$

where Γ is the incomplete gamma function. The integral is sensitive to the choice of L_{min} , especially for small β , so we explore a range of L_{min} . The incomplete gamma function was calculated using Mathematica (v. 4.0.1.0).

⁵In this paper, we use $H_0 = 75 \text{ km s}^{-1} \text{ Mpc}^{-1}$, $q_0 = 0.5$ cosmology.

Strong $H\alpha$ emission is an indicator of high star-formation rates and starburst activity. Therefore, the luminosity function of starburst galaxies was assumed to follow an $H\alpha$ luminosity function. At $z = 1.3$, Yan et al. (1999) find $\alpha = -1.35$, $\Phi^* = 1.7 \times 10^{-3} \text{ Mpc}^{-3}$, and $L^* = 7 \times 10^{42} \text{ ergs s}^{-1}$.

In Equation 2 and 3, the factor C_t arises because the cold gas causing the Mg II absorption is expected to remain after the outflow has ceased and the galaxy is no longer visible in $H\alpha$. We parameterize this as $C_t = \tau/t_{H\alpha}$, where τ is the time over which one can observe very strong absorption from the superwind and $t_{H\alpha}$ is the ratio of the lifetime of the symmetric-inverted systems to the lifetime of the $H\alpha$ luminosity.

Plugging Equation 3 into Equation 1 and using $N(z) = 0.15$ and $C_f = 1$, we obtain a family of C_t vs. L_{min}/L^* curves, which we present in Figure 2. We place C_t and L_{min} on the axes because they are the most uncertain parameters (see § 5). If values are chosen for R^* , α , and β , the C_t and L_{min} values necessary to produce $N(z) = 0.15$ can be read from the curves. Separate panels are shown for $R^* = 2, 5, 10$, and 20 kpc and the curves shown are for $\beta = 0, 0.05, 0.1$, and 0.15 . Note that a change in β by an amount $\Delta\beta$ is equivalent to a change in α by an amount $2\Delta\beta$.

5. CONSTRAINING PARAMETER SPACE

Theoretical models and observations of local superwinds can provide us with reasonable approximations of β , R^* , C_t , and L_{min} for comparison to our results in Figure 2.

5.1. Timescale

The $H\alpha$ luminosity will persist as long as there is a steady flow of ionizing photons from the nucleus of the starburst. Therefore, the $H\alpha$ luminosity should last as long as the O and B stars producing the starburst and driving the superwind ($\sim 10^7$ years). The timescale for Mg II absorption must be at least this long because it is observed in the post-starburst dwarf, NGC1705. The low-ionization gas will certainly persist for longer than this, but diffusion will eventually cause the material to spread out enough that the very strong Mg II systems are no longer seen. The timescale for this is not known exactly, but it is probably at least a few times the age of the starburst. The reason that we have used C_t as the ordinate of Figure 2 is because it is one of the most uncertain parameters.

5.2. Minimum Luminosity

We can place a constraint on L_{min} by again considering NGC1705, which has an $H\alpha$ luminosity of $\log(L_{H\alpha}/L^*) = -2.7$ (Marlow et al. 1997). Though NGC1705 is a starburst known to produce Mg II absorption over a large velocity spread, it has not been observed along a background quasar line of sight and we cannot be certain that a black-bottomed profile with a central inversion would be produced. Therefore, we explore a range of $-3.5 < \log L_{min} < -1.5$, allowing for uncertainty in either direction. In Figure 2, the curves rise dramatically (and require large C_t) at high L_{min} , so we expect that, to produce $N(z) = 0.15$, $\log L_{min}$ must be less than about -2.5 .

5.3. Radius-Luminosity Slope

The similarity solution of Mac Low & McCray (1988) predicts $R \propto L^{0.2}$ for an expanding superbubble, where L is the total luminosity of the early-type stars driving the bubble. Most of this luminosity will be hydrogen-ionizing, so one would expect $R \propto L_{H\alpha}^{0.2}$ as well. The later stages of the superwind (post-

blowout), however, cannot be treated as an expanding superbubble. At this point in the evolution of the superwind, the outflowing material is no longer being accelerated away from the galaxy but is, rather, being decelerated by ram pressure from the intergalactic medium (IGM) and by the galaxy potential well. Post-blowout outflows in more massive (and therefore more luminous) galaxies will have higher-velocity outflows, resulting in greater ram pressure from the IGM. More massive galaxies would also experience greater gravitational deceleration. Both of these effects act to decrease the radius-luminosity slope to $\beta < 0.2$. We only plot curves for $0 \leq \beta \leq 0.15$ in Figure 2 because the material will probably disperse before it has been significantly decelerated. Lower values of β produce more absorbers because they imply that the Holmberg relation is flat ($\beta \sim 0$) and the total cross section is being dominated by the large numbers of dwarf galaxies at the faint end of the luminosity function.

5.4. Radius-Luminosity Normalization

The Na I absorption radii of far-IR-bright starburst galaxies can be used to estimate plausible values of R^* for Mg II. Absorption in Na I is known to occur out to radii of 5 kpc with $C_f = 1$ (Heckman et al. 2000). The radii are lower limits because the background starlight becomes too faint beyond this point and because Mg II may exist out to a larger radius than Na I. If we are conservative and take $R^* = 5 \text{ kpc}$, we require a low L_{min} and/or a high C_t . There is reason to believe, however, that the absorption will be seen at larger radii. In a low-resolution spectrum, Norman et al. (1996) detected $W_r = 1.7 \text{ \AA}$ Mg II absorption at an impact parameter of 26 kpc from a starburst galaxy, but it is not known whether the system has the type of kinematic structure we are observing at high redshift. Also, $H\alpha$ emission has been seen out to an impact parameter of 11 kpc in M82 (Devine & Bally 1999), indicating the presence of cold material out to that radius. Radii of 10 kpc or greater will produce the observed $N(z)$ for moderate L_{min} and C_t factors of a few.

5.5. Summary

We expect $1 \lesssim C_t \lesssim 5$ based on the speed and duration of the superwind. Although we can't place a useful constraint on L_{min} from physical considerations, we argue $0 \lesssim \beta < 0.2$ by considering the pressure mechanisms acting on the expanding superbubble. Observations of local starburst galaxies tell us that $5 \lesssim R^* \lesssim 25$.

Using these physical arguments, we can further constrain parameter space by examining Figure 2. In order to obtain $N(z) = 0.15$ for reasonable values of C_t , we expect that $R^* \sim 10 \text{ kpc}$ and $\log L_{min} \lesssim -2.5$. The calculation is not particularly sensitive to β within the chosen range, so we can't place any further constraint on it from Figure 2. The timescale factor (C_t) cannot be constrained from Figure 2 either.

It should be recognized that the calculations presented here are very rough. We can only determine that the parameters needed to produce the observed $N(z)$ of $W_r > 1.8 \text{ \AA}$ Mg II absorption systems are consistent with the expected properties of superwinds at $z \sim 1.3$.

6. DISCUSSION

6.1. $N(z)$ of Lyman break Galaxies

High-redshift analogs of local superwinds, Lyman break galaxies, have been seen by Steidel et al. (1996) at $z \sim 3$.

A rest-frame ultraviolet spectrum of a lensed Lyman break galaxy, MS 1512-cB58, shows evidence for an outflow of $\sim 200 \text{ km s}^{-1}$ and a star formation rate of $\sim 40 \text{ M}_{\odot} \text{ yr}^{-1}$. These properties are similar to those we expect for the objects giving rise to the very strong MgII absorbers, indicating that MgII absorption could be used as a tracer of Lyman break galaxies at $z \sim 3$.

Using equation 1 and existing data on Lyman break galaxies, we can estimate the expected redshift number density of MgII absorbers from Lyman break galaxies. If we assume that these objects are like the $z \sim 1.3$ very strong MgII absorbers and use $R^* = 5 \text{ kpc}$ (see Section 5) as the typical absorption radius, we get $\sigma \simeq 80 \text{ kpc}^2$. The number density of Lyman break galaxies is $n \gtrsim 0.02 \text{ Mpc}^{-3}$ (Adelberger et al. 1998). This is a lower limit because it only takes into account those Lyman break galaxies that have been detected using photometric methods. Using equation 1, we get $N(z)_{LBG} \gtrsim 0.05$ at $z = 3$.

6.2. Superwind Contribution to Damped Lyman-Alpha Absorbers

The idea that superwinds seen in absorption might constitute a non-negligible fraction of the damped Ly α absorbers (DLAs, $\log N(\text{HI}) > 20.3 \text{ cm}^{-2}$) in quasar spectra was first proposed by Nulsen et al. (1998). Based on a rough model of a weakly collimated, biconical outflow, they determined that superwinds could give rise to the majority of DLAs at all redshifts. We assess whether the majority of symmetric-inverted ($W_r > 1.8 \text{ \AA}$) MgII profiles that we attribute to superwinds could also be DLAs.

Of the absorbers shown in Figure 1, two have measured HI column densities. The system in Q1213 - 0017 at $z = 1.5541$ was found not to be a DLA (Rao & Turnshek 2000) from analysis of a *HST/FOS* spectrum. For the system in Q1225 + 317 at $z = 1.7948$, a limit of $N(\text{HI}) < 5 \times 10^{18}$ was inferred from the lack of damping wings in an *IUE* spectrum (Bechtold et al. 1987). Thus, 50 % of the HIRES/Keck very strong MgII absorption systems have known HI column densities and both of them are not DLAs.

Rao & Turnshek (2000) searched for DLAs in the *HST/FOS* spectra of 87 MgII-absorption systems. Of the 87 MgII absorbers in their sample, nine of them have $W_r > 1.8 \text{ \AA}$. Of those nine absorbers, four are at $z > 1$. In total, 4/5 (80 %) of the $z < 1$ absorbers are DLAs, and 1/4 (25 %) of the $z > 1$ absorbers are DLAs. This suggests not only that the $z > 1$ very strong MgII systems are a different population than the

$z < 1$ systems, but that the $z > 1$ population displays a relative paucity of DLAs. Furthermore, in contrast to both superwinds and very strong MgII absorption systems, DLAs display no significant evolution in $N(z)$ from $z = 4$ to $z = 0$ (Rao & Turnshek 2000; Churchill 2001). If, as we hypothesize, superwinds give rise to the majority of $z > 1$, $W_r > 1.8 \text{ \AA}$ MgII absorbers, we are compelled to conclude that most DLAs are not superwinds.

Why might this be the case? Although large amounts of material ($\sim 60 \text{ M}_{\odot} \text{ yr}^{-1}$) are expelled in a superwind, the majority of this material is highly ionized (e.g. Tomisaka & Bregman 1993, Suchkov 1994, Strickland 1998, Tenorio-Tagle & Munoz-Tunon 1998). The only clouds that give rise to low-ionization absorption are the dense clouds of entrained material. High-equivalent width systems like the ones presented in Figure 1 could be produced with only small numbers of moderate-column density clouds (greater than about five) because the clouds in a superwind have a significant spread in velocity space ($\sim 300 \text{ km s}^{-1}$). It has been shown that the majority of DLAs have total velocity spreads less than 200 km s^{-1} (Prochaska & Wolfe 1999; Pettini et al. 2000), indicating that they are typically produced in environments less active than those which produce the very strong MgII absorbers. Figure 3 illustrates these differences. The bottom two panels contain high-resolution MgII profiles of two DLAs (Churchill et al. 2000b) and the top two panels show examples of symmetric-inverted MgII profiles from our sample.

7. CONCLUSION

The majority of very strong ($W_r > 1.8 \text{ \AA}$), $z > 1$ MgII absorption profiles with high-resolution spectra show distinctive kinematic features, including a central inversion and a large velocity spread. All of these features can be explained with a line of sight through a superwind. The redshift number density of absorbers expected from superwinds, $N(z)$, was calculated using parameters observed in local superwinds and was found to be consistent with the $N(z)$ of very strong MgII absorbers.

In addition, the absence of very strong MgII absorbers is consistent with the decrease in star formation from $z = 1$ to the present. The number of DLAs, however, is consistent with no evolution over this redshift range. In addition, the very strong MgII absorbers at $z > 1$ with known HI column densities display a paucity of DLAs as compared with the low-redshift very strong MgII absorbers, suggesting that the majority of DLAs do not arise in superwinds.

REFERENCES

- Adelberger, K. L., Steidel, C. C., Giavalisco, M., Dickinson, M., Pettini, M., & Kellogg, M. 1998, *ApJ*, 505, 18
 Bechtold, J., Green, R. F., & York, D. G. 1987, *ApJ*, 312, 50
 Charlton, J. C. & Churchill, C. W. 1998, *ApJ*, 499, 181
 Churchill, C. W. 1997, Ph.D. Thesis, University of California, Santa Cruz
 Churchill, C. W. 1999, in "Clustering at High Redshift", Proceedings from the ASP Conference Series 1999; eds. Mazure, A., Le Fèvre, O., & Le Brun, V.
 Churchill, C. W. 2001, *ApJ*, 560, in press (astro-ph/0105044)
 Churchill, C. W., Mellon, R. R., Charlton, J. C., Jannuzi, B. T., Kirhakos, S., Steidel, C. C., & Schneider, D. P. 1999, *ApJ*, 519, L43
 Churchill, C. W., Mellon, R. R., Charlton, J. C., Jannuzi, B. T., Kirhakos, S., Steidel, C. C., & Schneider, D. P. 2000a, *ApJS*, 130, 91
 Churchill, C. W., Mellon, R. R., Charlton, J. C., Jannuzi, B. T., Kirhakos, S., Steidel, C. C., & Schneider, D. P. 2000b, *ApJ*, 543, 577
 Churchill, C. W., Rigby, J. R., Charlton, J. C., & Vogt, S. S. 1999, *ApJ*, 120, 51
 Churchill, C. W., Steidel, C. C., & Vogt, S. S. 1996, *ApJ*, 471, 164
 Churchill, C. W. & Vogt, S. S. 2001, *AJ*, 122, in press (astro-ph/0106006)
 Danks, A. C., Walborn, N. R., Vieira, G., Landsman, W. B., Gales, J., & Garcia, B. 2001, *ApJ*, 547, L155
 Devine, D. & Bally, J. 1999, *ApJ*, 510, 197
 Guillemin, P., Bergeron, J. 1997, *A&A*, 328, 499
 Heckman, T. M. 2000, in "Gas and Galaxy Evolution", Proceedings from the ASP Conference Series 2000, eds: Hibbard, J. E., Rupen, M. P. & von Gorkom, J. H.
 Heckman, T. M., Armus, L., & Miley, G. K. 1990, *ApJS*, 74, 833
 Heckman, T. M., Lehnert, M. D., Strickland, D. K., & Armus, L. 2000, *ApJ*, 129, 493
 Heckman, T. M., Sembach, K. R., Meurer, G. R., Strickland, D. K., Martin, C. L., Calzetti, D., & Leitherer, C. 2001, *ApJ*, in press (astro-ph/0102283)
 Heckman, T. M., Sembach, K. R., & Leitherer, C. et al. 2001, in prep.
 Holmberg, E. 1975, in *Galaxies and the Universe*, ed. A. Sandage, M. Sandage, & J. Christian (Chicago: University of Chicago Press), 123
 Jenkins, E. B. 1996, *ApJ*, 471, 292
 Lanzetta, K. M., Wolfe, A. M., & Turnshek, D. A. 1987, *ApJ*, 322, 739
 Liu, M. C., Dey, A., Graham, J. R., Bundy, K. A., Steidel, C. C., Adelberger, K., & Dickinson, M. E. 2000, *AJ*, 119, 2556
 Lu, L., Sargent, W. L. W., & Barlow, T. A. 1996, *ApJ*, 107, 475
 Mac Low, M.-M., & McCray, R. 1988, *ApJ*, 324, 776
 Marlowe, A. T., Meurer, G. R., Heckman, T. M., & Schommer, R. 1997, *ApJS*, 112, 285

- Norman, C., Bowen, D., Heckman, T. M., Blades, J. C., & Danly, L. 1996, *ApJ*, 472, 73
- Nulsen, P. E. J., Barcons, X., Fabian, A. C. 1998, *MNRAS*, 301, 168
- Pettini, M., Steidel, C. C., Adelberger, K. L., Dickinson, M., & Giavalisco, M. 2000, *ApJ*, 528, 96
- Prochaska, J. X. & Wolfe, A. M. 1999, *ApJS*, 121, 369
- Rao, S. M. & Turnshek, D. A. 2000, *ApJ*, 130, 1
- Savage, B. D. & Sembach, K. R. 1991, *ApJ*, 379, 245
- Schechter, P. 1976, *ApJ*, 203, 297
- Sembach, K. R. & Savage, B. D. 1992, *ApJS*, 83, 147
- Steidel, C. C., Giavalisco, M., Dickinson, M., & Adelberger, K. L. 1996, *AJ*, 112, 352
- Steidel, C. C. & Sargent, W. W. 1992, *ApJS*, 80, 1
- Strickland, D. K. 1998, Ph.D. thesis, Univ. Birmingham
- Suchkov, A. A., Balsara, D. S., Heckman, T. M., & Leitherer, C. 1994, *ApJ*, 430, 511
- Tenorio-Tagle, G. & Munoz-Tunon, C. 1998, *MNRAS*, 293, 299
- Tomisaka, K., & Bregman, J. 1993, *PASJ*, 45, 513
- Tytler, D., Boksenberg, A., Sargent, W. L. W., Young, P., & Kunth, D. 1987, *ApJ*, 234, 33
- Vogt, S. S., et al. 1994, in *Proc. SPIE Conf. 2198, Instrumentation in Astronomy VII*, edited by D. L. Crawford and E. R. Craine (SPIE, Bellingham, WA), p. 362
- Yan, L., McCarthy, P. J., Freudling, W., Teplitz, H. I., Malumuth, E. M., Weymann, R. J., & Malkan, M. A. 1999, *ApJ*, 519, L47

TABLE 1
JOURNAL OF OBSERVATIONS

Object	V [mag]	z_{em}	Date [UT] ^a	Exp [s] ^b	λ Range [\AA]	Decker	Blocker
Q 0450 – 132	17.5	2.253	1995 Jan 24	5400	3986.5–6424.5	7''	kv370
Q 1213 – 003	17.0	2.691	1995 Jan 24	5200	5008.1–7356.7	14''	kv418
B2 1225 + 317	15.9	2.219	1995 Jan 24	2400	5737.5–8194.7	14''	og530

TABLE 2
ABSORBER PROPERTIES

Ion/Tran	$W_r, \text{\AA}$	N_a, cm^{-2}
Q 0450 – 132 $z_{\text{abs}} = 1.1746$ $\Delta v = 296 \text{ km s}^{-1}$		
Mn II 2577	0.14 ± 0.05	12.87 ± 0.02
Mn II 2594	0.09 ± 0.04	
Mn II 2606	0.06 ± 0.04	
Fe II 2261	0.13 ± 0.04	14.99 ± 0.03
Fe II 2344	0.77 ± 0.02	
Fe II 2374	0.49 ± 0.03	
Fe II 2383	1.07 ± 0.02	
Fe II 2600	1.15 ± 0.02	
Mg II 2796	1.82 ± 0.02	> 14.07
Q 1213 – 003 $z_{\text{abs}} = 1.3201$ $\Delta v = 397 \text{ km s}^{-1}$		
Mn II 2577	< 0.08	< 11.77
Mn II 2606	< 0.07	
Fe II 2344	1.07 ± 0.09	14.53 ± 0.02
Fe II 2374	0.42 ± 0.07	
Fe II 2383	1.67 ± 0.06	
Fe II 2587	0.88 ± 0.07	
Fe II 2600	1.59 ± 0.03	
Mg II 2796	2.79 ± 0.02	> 14.53
Mg II 2803	2.51 ± 0.02	
Mg I 2853	0.69 ± 0.05	12.84 ± 0.01
Q 1213 – 003 $z_{\text{abs}} = 1.5541$ $\Delta v = 430 \text{ km s}^{-1}$		
Mn II 2594	< 0.06	< 12.18
Mn II 2606	< 0.09	
Fe II 2261	0.02 ± 0.05	14.40 ± 0.01
Fe II 2344	0.50 ± 0.06	
Fe II 2374	0.28 ± 0.05	
Fe II 2383	0.85 ± 0.05	
Fe II 2587	0.46 ± 0.06	
Fe II 2600	0.85 ± 0.05	
Mg II 2796	1.99 ± 0.03	> 14.19
Mg II 2803	1.48 ± 0.04	
Mg I 2853	0.22 ± 0.08	12.31 ± 0.03
B2 1225 + 317 $z_{\text{abs}} = 1.7948$ $\Delta v = 343 \text{ km s}^{-1}$		
Mn II 2577	< 0.04	12.13 ± 0.14
Mn II 2606	< 0.05	
Fe II 2344	0.30 ± 0.04	13.88 ± 0.01
Fe II 2374	0.09 ± 0.04	
Fe II 2383	0.66 ± 0.03	
Fe II 2600	0.62 ± 0.05	
Mg II 2796	2.01 ± 0.02	> 14.29
Mg II 2803	1.59 ± 0.03	
Mg I 2853	0.28 ± 0.05	12.40 ± 0.02

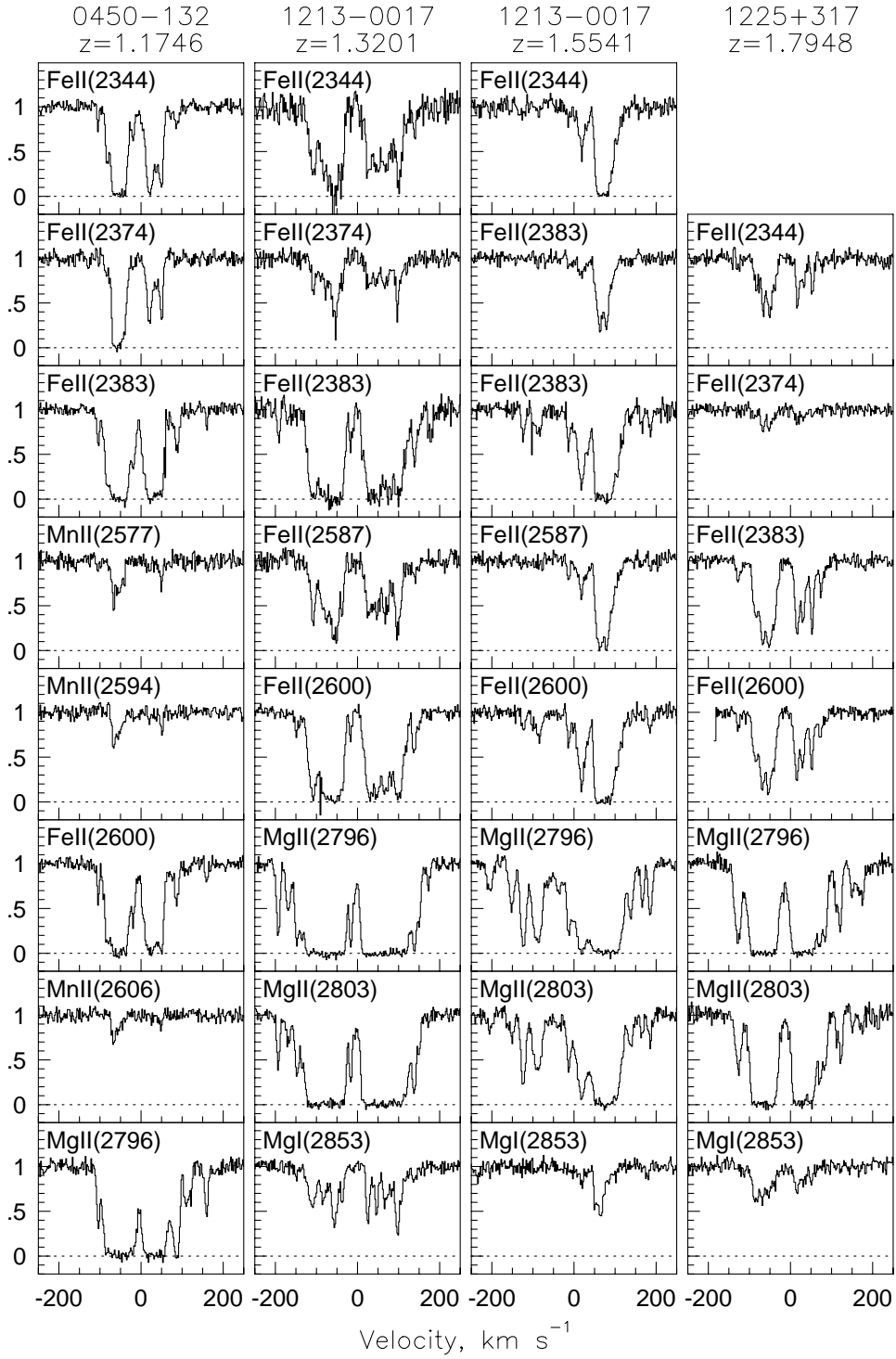


FIG. 1.— Four $W_r > 1.8 \text{ \AA}$ MgII absorption systems at $1 < z < 2$. The MgII $\lambda\lambda 2796, 2803$ doublet and the corresponding detected FeII, MgI, and MnII transitions are plotted, aligned in rest-frame velocity. The MgII 2803 transition was not covered in the spectrum of Q 0450 - 132. Data were obtained at $R \sim 6.6 \text{ km s}^{-1}$ with the HIRES spectrograph on the Keck I telescope.

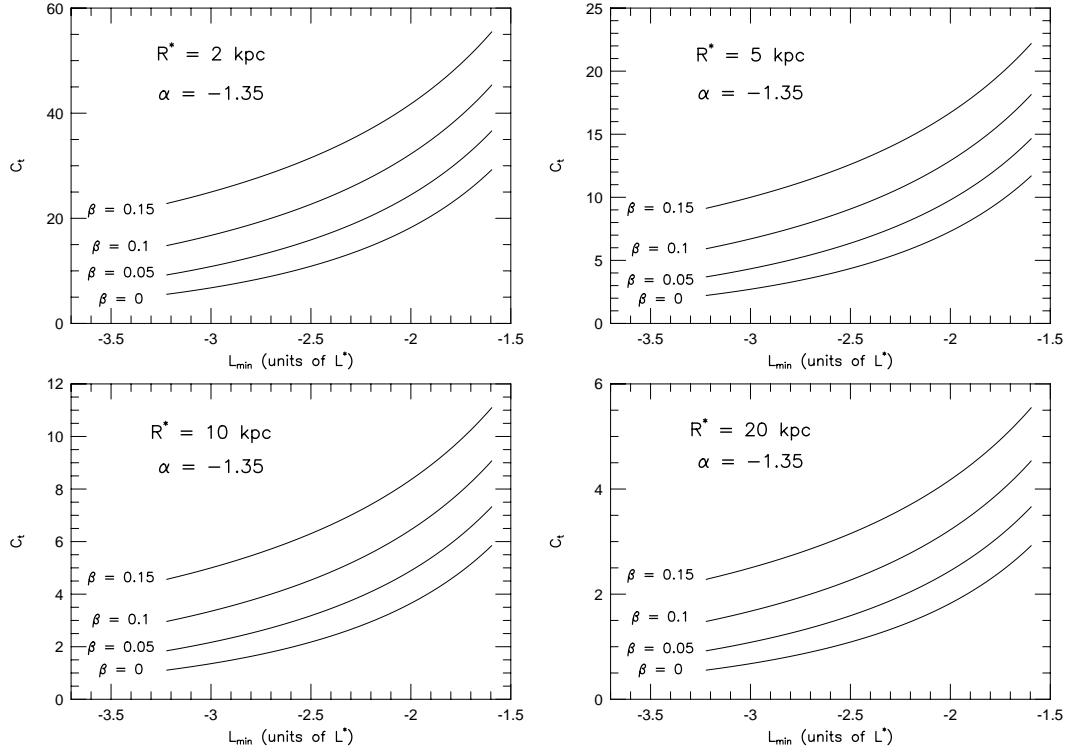


FIG. 2.— Plots of the parameters required to produce the observed number of MgII absorbers per unit redshift ($N(z)$) with $W_r > 1.8 \text{ \AA}$. Each curve represents the parameters (C_t and L_{min}) needed to produce the observed $N(z) = 0.16$ for a given R^* and β . The vertical axis gives the absorption timescale factor (C_t) and the horizontal axis, the minimum H α luminosity (L_{min}) for which very strong MgII absorption would be observed. Each plot assumes a different scale radius (R^*) for the radius–luminosity relation, $R = R^* (L/L^*)^\beta$, and curves are presented for different values of β as labelled.

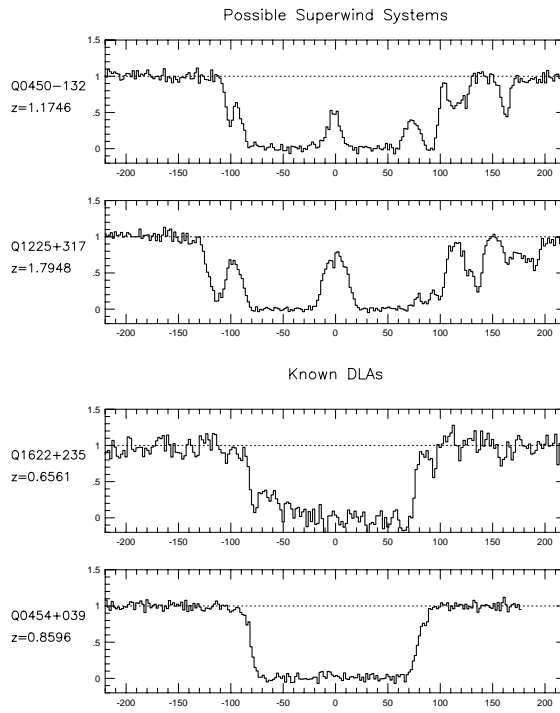


FIG. 3.— The top two panels show normalized Mg II 2796 absorption profiles for two characteristic $W_r > 1.8 \text{ \AA}$ profiles at $z > 1$. The profiles show a central inversion, as would be expected if the line of sight were passing through a superwind. The lower two panels show very strong Mg II absorbers at $z < 1$ that are also damped Ly α absorbers. The DLA systems show a single saturated Mg II absorption region and no central inversion.